

# ZnO Doped Graphite Nanocomposite via *Agathosma Betulina* Natural Extract with Improved Bandgap and Electrical Conductivity

**Thema FT<sup>1, 2\*</sup>, Ishaq A<sup>3</sup>, Ahmad RH<sup>3</sup>, Arshad M<sup>3</sup>, Ali NZ<sup>3</sup>, Mathe-ur-Rahman<sup>4</sup> and Maaza M<sup>1, 2</sup>**

<sup>1</sup>Unesco-Unisa Africa Chair in Nanosciences/Nanotechnology Laboratories, University of South Africa, South Africa

<sup>2</sup>Materials Research Department, Nanosciences African network, National Research Foundation (NRF), South Africa

<sup>3</sup>Nanoscience and Technology Department, National Centre for Physics, Pakistan

<sup>4</sup>Federal Urdu University of Arts, Science and Technology Islamabad, Pakistan

**\*Corresponding author:** Force Tefo Thema, Unesco-Unisa Africa Chair in Nanosciences/ Nanotechnology Laboratories, College of Graduate Studies, University of South Africa (UNISA), Muckleneuk Ridge, P O Box 392, Pretoria, South Africa, Tel: +27 (0) 21 843 1149; E-mail: ftthema@gmail.com

## Research Article

Volume 2 Issue 3

**Received Date:** November 09, 2017

**Published Date:** November 20, 2017

**DOI:** 10.23880/nnoa-16000129

## Abstract

This contribution reports for the first time on green synthesized Zinc Oxide graphite doped (ZnO/G) material that was fabricated and exposed to UV lamp irradiation at 250 nm for 4 hrs. The morphology and the structure of ZnO and ZnO/G were characterized by high resolution transmission electron (HRTEM) and X-ray diffraction (XRD) respectively. The Energy Dispersive spectroscopy (EDS) confirms the purity of ZnO nanoparticles which is substantiated by the XPS spectrum. Diffuse Reflectance spectroscopy (DRS) reveals decrease in bandgap and reflectance of the irradiated composite with (I-V) character curve showing enhanced ZnO/G electrical conductivity.

**Keywords:** *Agathosma Betulina* Natural Extract; Zinc Oxide Nanoparticles; Graphite; Bandgap; Composite And Electrical Conductivity

## Introduction

Recently, there has been significant edge in research related to preparation, characterization and application of

metal oxide nanoparticles with desired properties [1]. Synthesis and characterization of nanomaterials with special morphology and specific structure are of fundamental importance [2-3]. In this light,

semiconductor particles that are in the nanometer size regime have attracted significant attention because of their atom like size dependent properties [4]. More precisely, Zinc Oxide (ZnO) also known as Zincite is one such promising oxide semiconductor material which shows good electrical, optical and piezo-electrical properties [5]. ZnO has direct wide band gap energy of 3.37 eV at room temperature and a large exciton binding energy (60 meV) [6]. It has similar wurtzite crystal structure and optical properties as those of GaN hence; it has attracted significant interest worldwide as a potential and ideal candidate for blue light emitting diodes applications. Relative to GaN, ZnO is sufficiently stable with a melting temperature of 2248 K [6]. It can withstand high temperature associated with doping and forming ohmic contacts. It has become one of the most important functional materials with unique properties of near-ultraviolet emission and optical transparency [7,8].

Zincite can therefore, be used in various applications such as solar cells, gas sensors and field-emission displays. Zinc Oxide nanomaterial is also used in thermal and quantum devices, in catalysis, electronic and in wastewater treatment as an adsorbent and photocatalyst [9,10]. Other technological applications like chemical remediation, photo initiation of polymerization reactions, quantum dot devices and solar energy conversion have been reported [11]. Various types of synthesis techniques such as solvo-thermal, hydrothermal, sol-gel, solution-combustion, sonochemical [12-14] have been done. It is therefore, fundamentally important that simple, cost effective, accessible, scalable and environment friendly method to synthesize nanomaterials be availed urgently. Hence, in this work, we have for the first time successfully synthesized ZnO via *Agathosma betulina* natural extract [6,15] which we doped with graphite to fabricate a composite with the aim of tuning and improving its bandgap.

## Experimental

### Zinc Oxide Sample Preparation via *Agathosma Betulina* Extract

The ZnO nanoparticles used in this work were produced as described or similar to the chemical reaction reported by Thema FT et al. [5] in our previous work.

### Preparation of the Composite (ZnO-G)

Graphite bay flakes was commercially bought and used with no further purification. 1:20 ratio by weight of graphite to green synthesized ZnO powder were physical mixed and ground together by a mortar and pestle. The resultant powder was dispersed in 50 ml of ethanol and sonicated for 2 hrs to produce uniform dispersion. The mixture was then exposed to a 500 W high pressure Hg lamp with main wave crest at 365 nm for about 4 hours under ambient conditions while stirring in a dark environment. The mixture was then filtered and dried at 35°C resulting into ZnO/G powder.

### Fabrication of the thin film

Fluorine Tin Oxide (FTO) was used as a substrate to fabricate ZnO and ZnO/G thin films. A mixture of distilled water, ethanol and acetic acid in a ratio (1:2:1) was prepared. In a 0.3g ZnO and ZnO/G powder, the mixture was dropped until the powder became pasty and ultra-sonicated in a bath to dissolve the nanoparticles. Finally, the novel doctor blade technique for deposition of thin film was done. In this technique, we used double tape to attach the non-conducting side of the substrate on the table while pasting the small amount of pasty material on The FTO substrate using the blade to spread the gel like material. The thin films were annealed at 400°C for 1 hrs in a furnace to enhance adhesion.

## Results & Discussion

### Morphological and Microscopy Observations

Figure 1 below reports on a typical High Resolution Transmission Electron Microscopy (TEM) image of annealed ZnO nanoparticles at 500°C. It consists of quasi-spherical agglomerated nanoscaled particles. The Selected Area Electron Diffraction (SAED) profile Figure 1a inset shows spotty ring patterns of highly crystalline structure of the ZnO nanoparticles. Figure 1b shows image of HRTEM of single nanoparticles revealing series of distinguished reticular planes with distances  $d_{hkl}$  of 0.25 nm and 0.28 nm. They fit well with (101) and (100) reticular distances of the ZnO hexagonal wurtzite structure JCPDS card (no. 00-036-1451).

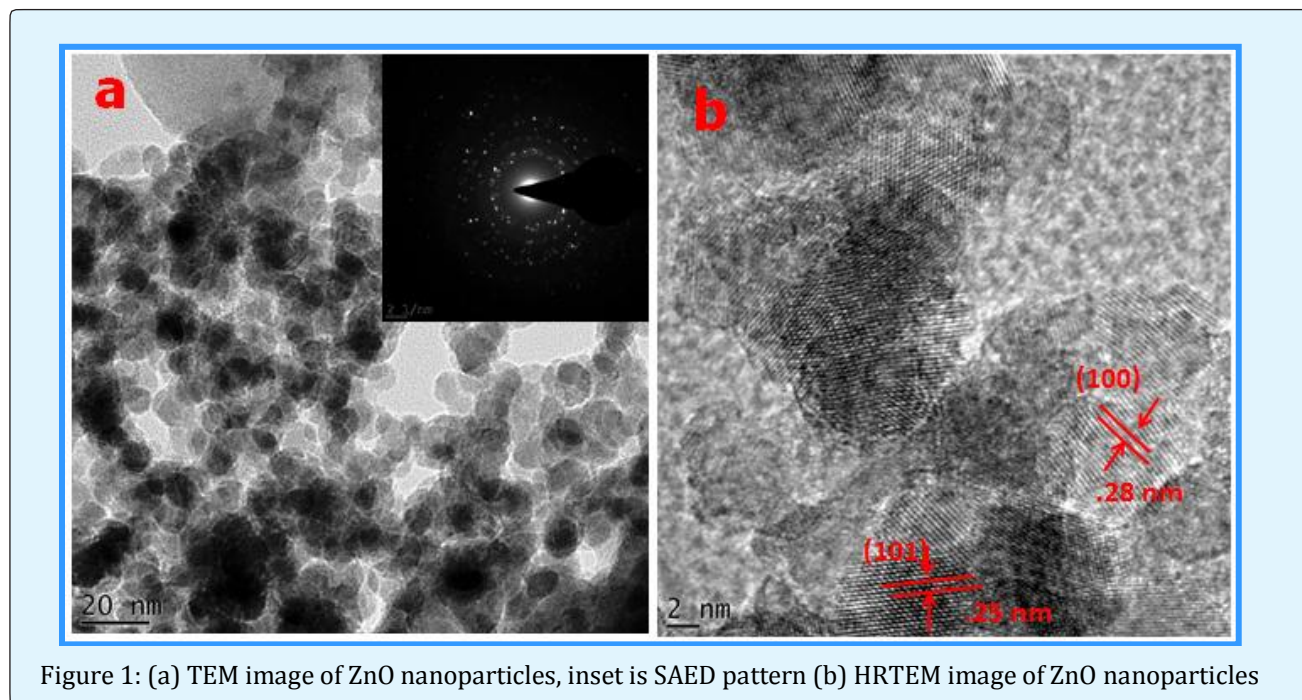


Figure 1: (a) TEM image of ZnO nanoparticles, inset is SAED pattern (b) HRTEM image of ZnO nanoparticles

### Elemental analysis

Figure 2 shows a typical Energy Dispersive spectroscopy (EDS) spectrum obtained from Oxford instruments X-Max solid state silicon drift detector at 20 keV on 500 °C annealed ZnO powder. It shows the purity of the green synthesized ZnO nanoparticles with appearances of Carbon and Copper which are a result of carbon coating and sample holder material respectively.

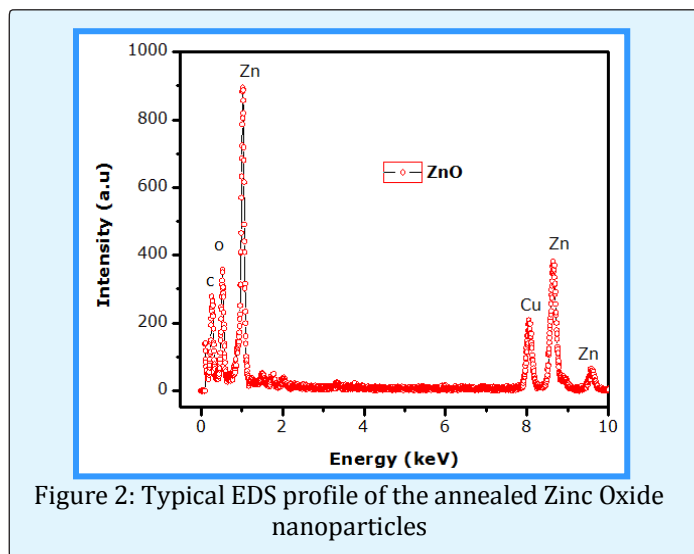


Figure 2: Typical EDS profile of the annealed Zinc Oxide nanoparticles

### Crystallographic analysis

The XRD study was carried on Bruker Advanced D8 diffractometer with monochromated Cu K $\alpha$  radiation of a wavelength 1.5406 Å operating at a current of 40 mA and a voltage of 40 kV in Bragg-Brentano geometry. Figure 3 shows the XRD profile obtained on the ZnO dried powder in a standard and nanomaterial annealed at 500°C. All the diffraction Bragg peaks of annealed nano-powder match well with the hexagonal structure of ZnO. The crystal structure exhibited by ZnO is wurtzite blende and rock salt or Rochelle salt. The X-ray diffraction (XRD) pattern of the annealed powders is shown by Figure 3 below where the Miller indices indicate each Bragg peak. The ZnO peaks are indexed as standard hexagonal wurtzite structure which confirm very well with the JCPDS card (no. 36-1451). No any other peaks appear confirming the purity of ZnO nanoparticles except the Carbon and Copper which are due to Carbon coating and Copper as a result of sample holder. This observation fits and concurs very well with the TEM-EDS data above. The protruding peak indexed (002) is purely a characteristic peak for graphite material in the composite.

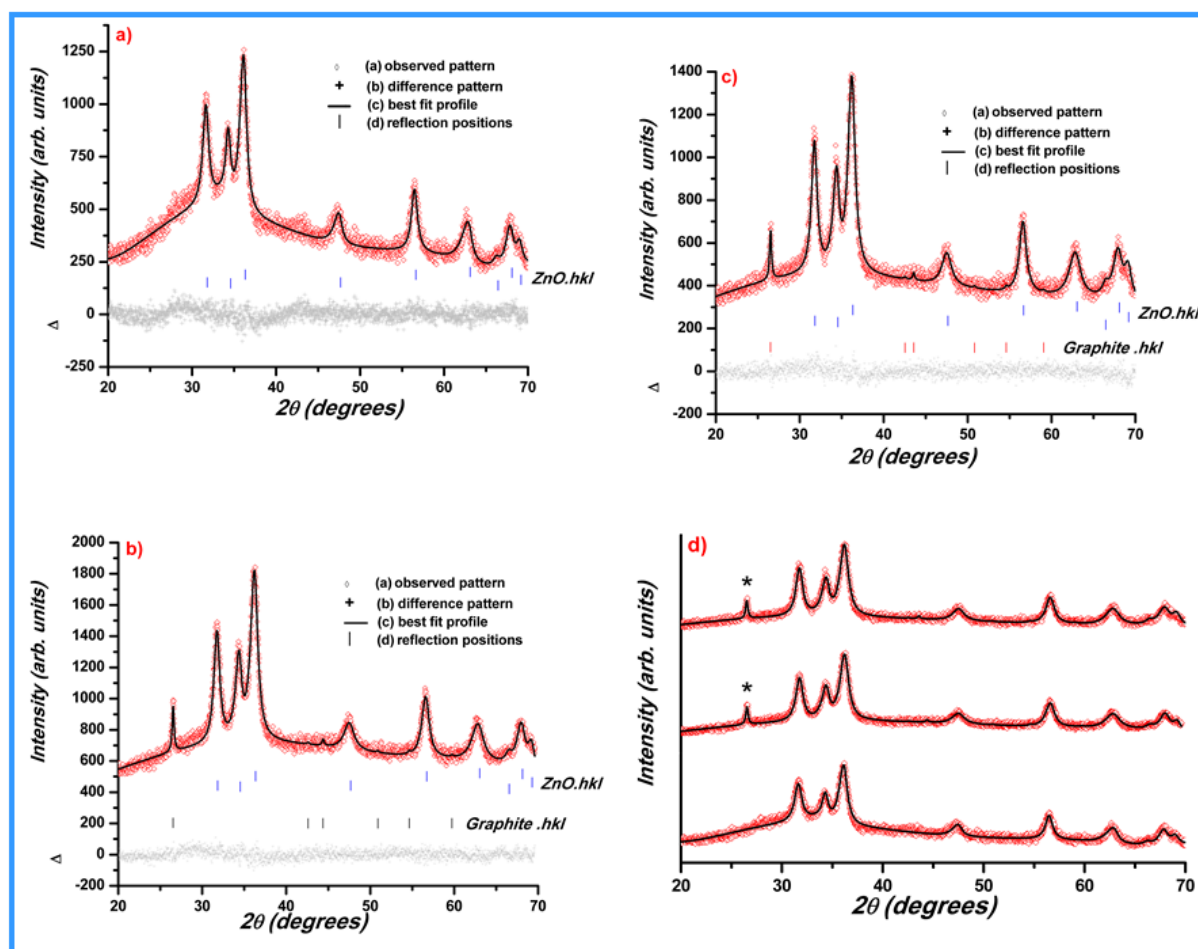


Figure 3: Scattered X-ray intensity for a polycrystalline sample of a) pure ZnO b) ZnO with Graphite c) ZnO with Graphite under UV, d) overlapped XRD patterns with asterisk (\*) highlighting the graphite reflections, depicting the observed pattern (diamonds), the best Rietveld-fit profile (black line), reflection markers (vertical bars), and difference plot  $\Delta = I_{\text{obs}} - I_{\text{calc}}$  (gray line) (shifted by a constant amount).

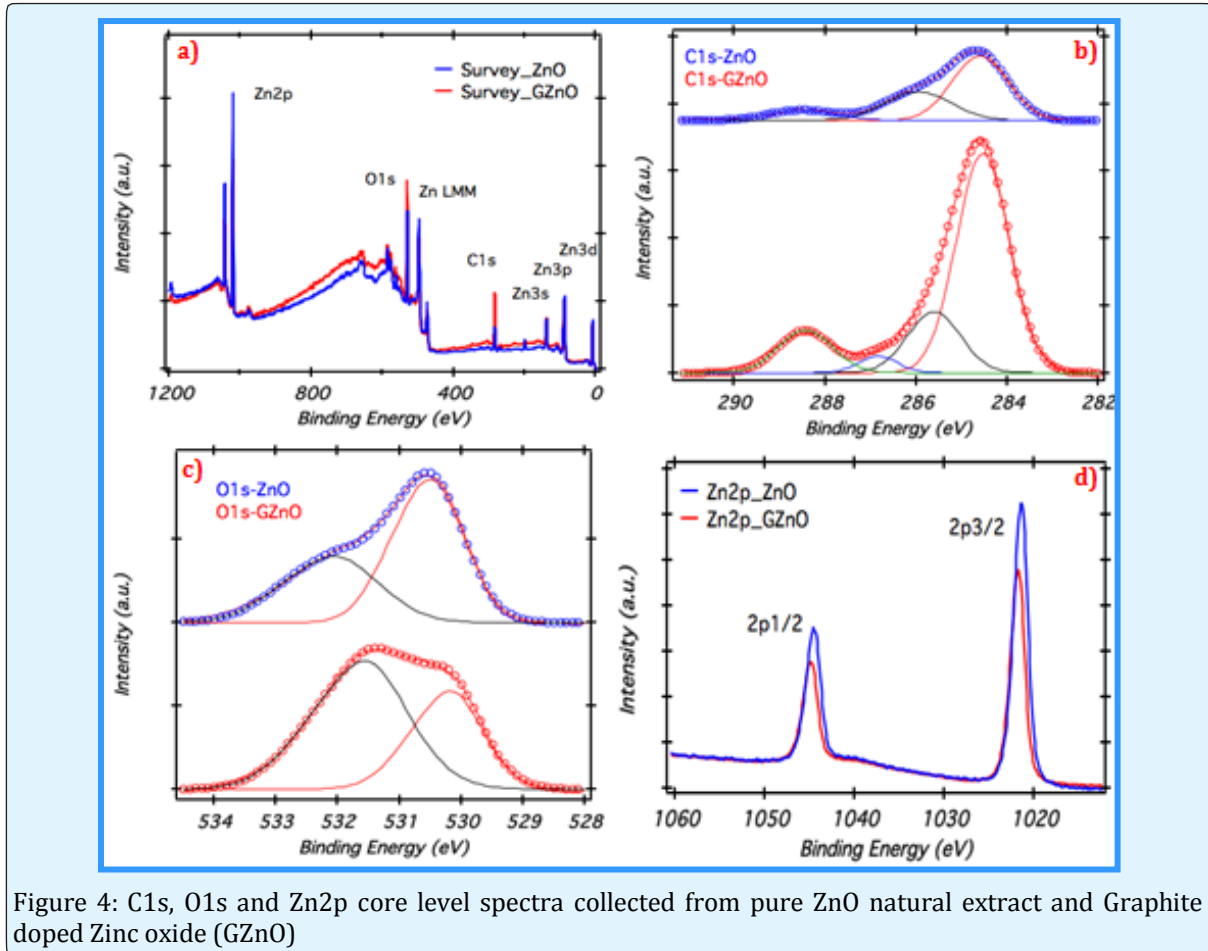
### X-ray Photoelectron Spectroscopy

The XPS spectra collected from pure Zinc Oxide and graphite doped Zinc Oxide is shown in Figure 4a. The survey scan was obtained to identify the elements present on the surface of the samples. The Carbon, Oxygen and Zinc along with Auger peaks were observed. C1s, O1s, and Zn2p spectra for comprehensive analysis of pure ZnO and Graphite doped ZnO are shown.

The C1s spectra obtained from pure ZnO is fitted with three peaks located at 284.5 eV, 286 eV and 288.5 eV, which are due to adventitious Carbon contamination corresponds to C-C, C-O-C and O-C=O respectively [20-22]. Figure 4b shows the C1s spectrum received from

graphite doped ZnO. The first peak at 284.6 eV is assigned graphitic Carbon (sp<sup>2</sup>), whereas, the peaks at higher binding energies at 285.8 eV, 287.3 eV and 288.5 eV are related to oxidized species [23]. The O1s peaks in Figure 4c for pure ZnO and Graphite doped is deconvoluted into two peaks. The first peak is located at  $530.3 \pm 0.1$  eV, which is assigned to O<sup>2-</sup> ions bounded by Zn in ZnO indicating fully oxidized atmosphere [24], while the second peak centered at  $531.7 \pm 0.2$  eV is allocated to oxygen vacancies within ZnO matrix. In Figure 4d Zn2p core level spectra for pure ZnO and graphite doped spectra are shown; The peaks for Zn2p<sub>3/2</sub> and 2p<sub>1/2</sub> are positioned at 1021.5 eV and 1044.6 eV respectively, which endorses the occurrence of Zinc in Zn<sup>+2</sup> state for

pure graphite doped ZnO samples [25].



### Bandgap tuning

Presence of band gap ( $E_g$ ) in nanoparticles shows its possible usage as a photocatalyst. ZnO is commonly used as a photo catalyst. UV visible DRS of the green synthesized ZnO nanoparticles was carried out as shown in Figure 5. Green synthesized nanoparticles (Figure 5) shows minimum reflectance in UV region at 380–400 nm which is often observed for ZnO photo catalysts.  $E_g$  value was calculated using Tauc plot (Figure 6) and was found to be 3.12 eV. Priyanka et al. [16] reported  $E_g$  value of 3.25 eV for pure ZnO while Dhiman et al. [17] found the  $E_g$  value of pure ZnO prepared by solution combustion method to be 3.30 eV. The Diffuse Reflectance spectroscopy (DRS) in Figure 5 indicates extremely significant reflectance decrease in the green synthesized ZnO particles after been doped with graphite. However, there is no much difference when the composite is exposed to UV irradiation for 4 hrs. There is only a slight shift observed as shown below.

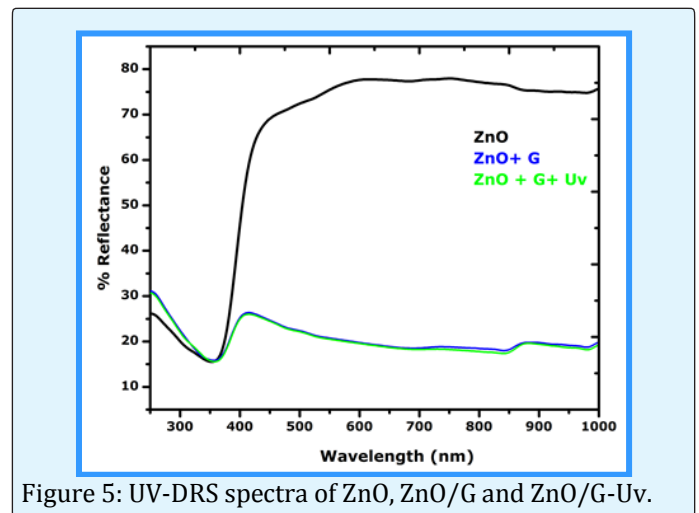


Figure 6 below shows that the green synthesized ZnO nanoparticles have a bandgap of 3.12 eV which is far much better than the reported bandgap of 3.67 eV from literature [6]. It is even interesting to see that after making a composite with graphite it improved from 3.12 eV to 3.07 eV with only a slight shift to 3.05 eV after irradiation with UV lamp.

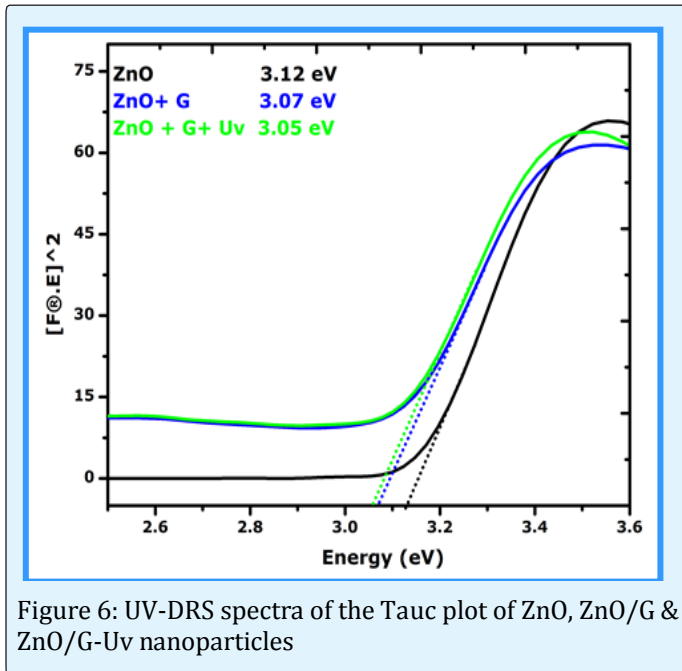


Figure 6: UV-DRS spectra of the Tauc plot of ZnO, ZnO/G & ZnO/G-Uv nanoparticles

### Electrical Conductivity

Figure 7 shows the current voltage (I–V) characteristics of Graphite, ZnO, and ZnO/G exposed to UV light for 4 hrs. The UV illumination was provided by a UV light emitting diode with a peak wavelength of 365 nm. Both reverse and forward currents increased due to the adsorption of UV light. The photo response of the graphite/ZnO composite was determined by oxygen desorption and absorption of electrons at the ZnO surface area.

oxygen molecules adsorbed on the surface move away with electrons from the conduction band of ZnO to form  $O_2^-$  &  $O^-$  anions. During this process, the formation of a depletion region with reduced carrier concentration near the sample surface [18] is created. When electron hole pairs are generated upon UV illumination, the photo generated holes migrate to the surface and discharge the adsorbed oxygen ions through surface electron hole recombination. Simultaneously, the photo generated electrons increase the total current of the devices [19].

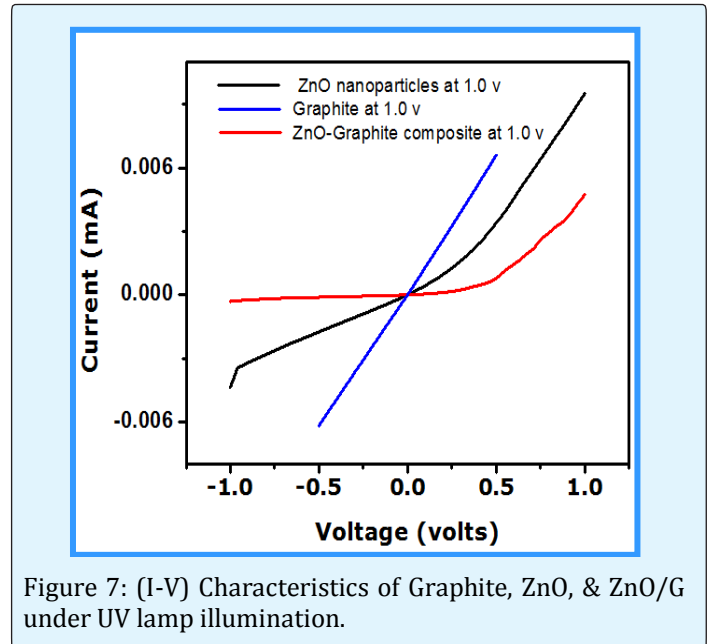


Figure 7: (I-V) Characteristics of Graphite, ZnO, & ZnO/G under UV lamp illumination.

### Conclusion

The synthesis of single highly crystalline ZnO has been achieved via green novel method which is environment friendly by using *Agathosma betulina* natural extract for the first time. Likewise, the resultant ZnO nanoparticles have been doped with graphite to tune and improve its bandgap. Interestingly, the ZnO/G composite under UV lamp demonstrated excellent electrical properties.

### Acknowledgements

This research program was generously supported by grants from the National Research Foundation of South Africa (NRF), the Unesco-Unisa Africa Chair in Nanosciences & Nanotechnology (Unesco-Unisa), iThemba LABS) as well as the National Centre for Physics (NCP), Islamabad, Pakistan to whom we are grateful.

### References

1. Moezzi A, McDonagh AM, Cortie MB (2012) Zinc oxide particles: Synthesis, properties and applications. *J Chem Eng* 185: 1-22.
2. Anjali P, Sonia TS, Imran Shakir, Shantikumar VN, Avinash Balakrishnan (2015) On the synthesis and electrochemical characterization of ordered hierarchical NiO micro bouquets with trimodal pore size distribution. *J Alloys Comp* 618: 396-402.

3. Lai M, Riley DJ (2006) Templated Electrosynthesis of Zinc Oxide Nanorods. *J Chem Mater* 18(9): 2233-2237.
4. Norifusa S, Toshio N, Kenta K, Kimihisa Y (2008) Quantum size effect in TiO<sub>2</sub> nanoparticles prepared by finely controlled metal assembly on dendrimer templates. *Nat Nanotechnol* 3: 106-111.
5. Thema FT, Manikandan E, Dhlamini MS, Maaza M (2015) Green synthesis of ZnO nanoparticles via *Agathosma betulina* natural extract. *Mater Lett* 161: 124-127.
6. Diallo A, Ngom BN, Park E, Maaza M (2015) Green synthesis of ZnO nanoparticles by *Aspalathus linearis*: Structural & optical properties. *J Alloys Comp* 646: 425-430.
7. Simon PFW, Ulrich R, Spiess HW, Wiesner U (2001) Block Copolymer-Ceramic Hybrid Materials from Organically Modified Ceramic Precursors. *Chem Mater* 13(10): 3464-3486.
8. Yu SH, Colfen H (2004) Bio-inspired crystal morphogenesis by hydrophilic polymers. *J Mater Chem* 14: 2124-2147.
9. Ding J, Wang M, Deng J, Gao W, Yang Z, et al. (2014) A comparison study between ZnO nanorods coated with graphene oxide and reduced graphene oxide. *J Alloys Comp* 582: 29-32.
10. Wahaba R, Hwangb IH, Kima YS, Shina HS (2011) Photocatalytic activity of zinc oxide micro-flowers synthesized via solution method. *Chem Eng J* 168(1): 359-366.
11. Zhanga Y, Sunb X, Pana L, Li H, Suna Z, et al. (2009) *J Alloys Comp* 480: 17-19.
12. Arkhireeva A, Hay JN, Lane JM, Manzano M, Masters H, et al. (2004) Synthesis of Organic-Inorganic Hybrid Particles by Sol-Gel Chemistry. *J Sol-Gel Sci Technol* 31(1-2): 31-36.
13. Kumar RV, Diamant Y, Gedanken A (2000) Sonochemical Synthesis and Characterization of Nanometer-Size Transition Metal Oxides from Metal Acetates. *Chem Mater* 12(8): 2301-2305.
14. Liang D, Cui C, Hub H, Wang Y, Xu S, et al. (2014) One-step hydrothermal synthesis of anatase TiO<sub>2</sub>/reduced graphene oxide nanocomposites with enhanced photocatalytic activity. *J Alloys Comp* 582: 236-240.
15. Thema FT, Beukes P, Gurib-Fakim A, Maaza M (2015) Green synthesis of Montepelite CdO nanoparticles by *Agathosma betulina* natural extract. *J Alloys Comp* 646: 1043-1048.
16. Priyanka, Srivastava VC (2013) Photocatalytic Oxidation of Dye Bearing Wastewater by Iron Doped Zinc Oxide. *Ind Eng Chem Res* 52(50): 17790-17799.
17. Dhiman P, Batoo KM, Kotnala RK, Singh M (2012) Fe-doped ZnO nanoparticles synthesised by solution combustion method. *micro & Nano Lett* 7(12): 1333-1335.
18. Yatskiv R, Grym J, Verde M (2015) Graphite/ZnO nanorods junction for ultraviolet photodetectors. *Solid State Electronics* 105: 70-73.
19. Nie BA, Hu JG, Luo LB, Xie C, Zeng LH, et al. (2013) Monolayer graphene film on ZnO nanorod array for high-performance Schottky junction ultraviolet photodetectors. *Small* 9(17): 2872-2879.
20. Jeong HK, Lee YP, Park MH, Kim IJ, Yang CW, et al. (2008) Evidence of graphitic AB stacking order of graphite oxides. *J Am Chem Soc* 130(4): 1362-1366.
21. Ganguly A, Sharma S, Papakonstantinou P, Hamilton J (2011) Probing the Thermal Deoxygenation of Graphene Oxide Using High-Resolution In Situ X-ray-Based Spectroscopies. *J Phys Chem C* 115(34): 17009-17019.
22. Guzman SS, Jayan BR, E de la Rosa, Castro AT, Gonzalez GV, et al. (2009) Synthesis of assembled ZnO structures by precipitation method in aqueous media. *Materials Chem & Phys* 115(1): 172-178.
23. Law JBK, Thong JTL (2008) Improving the NH<sub>3</sub> gas sensitivity of ZnO nanowire sensors by reducing the carrier concentration. *Nanotechnology* 19: 205502.
24. Strohmeier BR, Hercules DM (1984) Surface spectroscopic characterization of the interaction between zinc ions and  $\gamma$ -alumina. *J Catalysis* 86(2): 266-279.
25. Lebugle A, Axelsson U, Nyholm R, Prtensson NM (1981) Experimental L and M Core Level Binding Energies for the Metals 22Ti to 30Zn. *Physica Scripta* 23(5A): 825-827.

